THEORY OF COHERENT RADIATION FROM A GRATING-WAVEGUIDE FREE-ELECTRON LASER

Yuan-Yao Lin and Yen-Chieh Huang

Institute of Photonics Technologies, National Tsinghua University, Hsinchu 30043, Taiwan

Abstract

A grating-waveguide free electron laser can function as a mirrorless distributed-feedback oscillator near the Bragg resonance, as well as a backward-wave oscillator and forward wave amplifier at the other portions of the dispersion curve. Low oscillation threshold and single longitudinal mode are expected from this type of relativistic distributed-feedback oscillator.

INTRODUCTION

Since Urata *et al.* [1] observed superradiant Smith-Purcell emission by using a 30-40 keV electron beam from a scanning electron microscope, there has been a wide interest in investigating high-gain THz Smith-Purcell radiators pumped by keV electron beams. A Smith-Purcell radiator produces transversely asymmetric spontaneous radiation due to the arrangement of a single grating on one side of the electron beam. This asymmetric output could limit the usefulness of such a device in the THz regime where diffraction of waves is severe. This problem is partially solved by the so-called planar orotron [2] in which a planar metallic plate is installed above a grating to form a wave-guiding structure. Killoran *et al.* [3] further developed a dual-grating resonator in which an electron beam propagates closer to one of two parallel gratings. The grating closer to the electron beam is used for generating Smith-Purcell radiation and the other is used for reflecting radiation of certain angles back to the driving electron beam.

We describe in this paper a grating-waveguide free-electron laser (FEL) with two planar gratings arranged in parallel to an axial electron beam. This arrangement is similar to a millimetre-wave backward wave oscillator (BWO) using a corrugated cylindrical waveguide. We propose in this paper that a grating-waveguide FEL operating at the Bragg resonance can be a low-threshold, mirrorless distributed-feedback (DFB) oscillator. In addition, this paper is to extend the BWO concept to a planar design suitable for generating THz radiations.

MODE ANALYSIS

To explain the superradiant Smith-Purcell emission observed by Urata *et al.*, Andrews *et al.* [4] has modelled the problem as enhance harmonic radiation from electron bunching when a moving plasma dielectric interacts with a surface evanescent wave. In the following, we adopt the plasma-dielectric approach for calculating the eigenmode and small-signal gain of a grating-waveguide FEL.

Figure 1 defines the coordinates and symbols in our calculation. In Fig. 1, two conducting gratings are arranged in parallel to each other with their grating

vectors aligned in the *z* direction. The two gratings do not have any variation in the *x* direction and form a waveguide for waves propagating in the *z* direction. The grating has a period Λ_g, groove depth *D*, and groove width *W*.
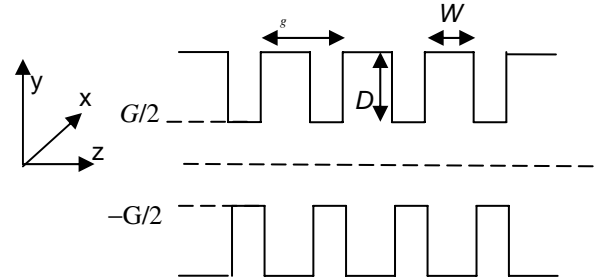
Figure 1: The structure of a grating-waveguide FEL. The variables Λ_g, *D*, *W*, and *G* are the grating period, groove depth, groove width, and grating gap, respectively. The electron beam propagates in *z*. The structure has no variation in *x*.

We assume that a uniform electron beam propagates in the *z* direction and fills up the waveguide-gap region between $-G/2 \leq y \leq G/2$. With this arrangement, only the TM wave in the waveguide needs to be considered. By using Floquet's theorem, the electric field intensity in the *z* direction E_z and the magnetic field intensity in the *x* direction H_x in the grating-gap region can be expanded as

$$E_z = \sum_{p=-\infty}^{\infty}[E_p^c \cosh(-\alpha_p y) + E_p^s \sinh(-\alpha_p y)]e^{-jp\mathrm{K}_g z}e^{j(\omega t - k_z z)} \quad (1)$$

$$H_x = \sum_{p=-\infty}^{\infty}[H_p^c \cosh(-\alpha_p y) + H_p^s \sinh(-\alpha_p y)]e^{-jp\mathrm{K}_g z}e^{j(\omega t - k_z z)} \quad (2)$$

where *p* is the index of the spatial harmonics, k_z is the wave number in the *z* direction for $p = 0$, $\mathrm{K}_g = 2\pi/\Lambda_g$ is the grating wave number, ω is the radiation frequency, and the superscripts *c* and *s* denote the symmetric and anti-symmetric distribution of the field components in the waveguide gap, respectively. With ω_p' being the plasma frequency in the electron rest frame, α_p is given by [4]

$$\alpha_p^{\;2} = (k_z + p\mathrm{K}_g)^2 - \frac{\omega^2}{c^2} + \frac{\omega_p'^{\;2}}{c^2} \quad (3)$$

From Ampere's law, Eqs. (1, 2) are coupled through the expressions

$$\alpha_p H_p^c = -j\omega\varepsilon E_p^s$$
$$\alpha_p H_p^s = -j\omega\varepsilon E_p^c \tag{4}$$

where $\varepsilon = \varepsilon_0(1+\chi'_p)$ is the permittivity of the plasma dielectric with the electric susceptibility

$$\chi'_p = -\frac{\omega_p^2}{\gamma^3(\omega - c\beta\cdot(k_z + pK_g))^2} \tag{5}$$

In Eq. (5), γ is the Lorentz factor, ω_p is the plasma frequency in the laboratory frame, and $\beta \equiv v/c$ with v and c being the electron speed and wave speed in vacuum, respectively. Because a uniform electron beam is strongly coupled to the symmetric E_z mode, we set $E_p^s = 0$ in Eq. (1) and thus $H_p^c = 0$ in Eq. (2) as a result of Eq. (4).

In the groove region where $-(G/2+D) \le y \le -G/2$ and $0 \le z \le W$ the electric field E_z and the magnetic field H_x can be expressed as

$$E_z = \sum_{n=0}^{\infty} \overline{E}_n \cos(\frac{n\pi z}{W})\frac{\sinh[\kappa_n(y+\frac{G}{2}+D)]}{\cosh(\kappa_n D)}e^{j\alpha} \tag{6}$$

$$H_x = \sum_{n=0}^{\infty} \overline{H}_n \cos(\frac{n\pi z}{W})\frac{\cosh[\kappa_n(y+\frac{G}{2}+D)]}{\sinh(\kappa_n D)}e^{j\alpha} \tag{7}$$

where the tangential electrical field E_z vanishes at the metal surface $y = -(G/2+D)$, and $E_y = -(j/\omega\varepsilon)(\partial H_x/\partial z)$ vanishes at both $z = 0$ and $z = W$. Also, $E_i(z+\Lambda_g) = e^{-jk_z\Lambda_g}E_i(z)$ and $H_i(z+\Lambda_g) = e^{-jk_z\Lambda_g}H_i(z)$ with $i = x,y,z$ must hold for the periodic boundary condition. From the wave equation, the coefficient κ_n satisfies

$$\kappa_n^2 = \left(\frac{n\pi}{W}\right)^2 - \frac{\omega^2}{c^2} \tag{8}$$

By matching the boundary condition at $y = \pm G/2$, one obtains

$$C_{nm} - \delta_{nm} = 0 \tag{9}$$

where

$$C_{nm} = \frac{-2\kappa_n}{W\Lambda_g(\delta_{n0}+1)}\tanh(\kappa_m D)\sum_{p=-\infty}^{\infty}\frac{1+\chi'_p}{\alpha_p}\tanh(\alpha_p\frac{G}{2})\Gamma_{pn}^-\Gamma_{pm}^+ \tag{10}$$

with $\begin{cases}\delta_{nm} = 1, & m = n \\ \delta_{nm} = 0, & \text{else}\end{cases}$, and

$$\Gamma_{pn}^+ = \frac{-j(pK_g + k_z)}{(pK_g + k_z)^2 - (\frac{n\pi}{W})^2}[(-1)^n e^{j(pK_g+k_z)W} - 1]$$

$$\Gamma_{pm}^- = \frac{-j(pK_g + k_z)}{(pK_g + k_z)^2 - (\frac{n\pi}{W})^2}[(-1)^n e^{-j(pK_g+k_z)W} - 1]$$

Eq. (9) is the dispersion relation and its solution $a(k)$ gives the guiding modes of this structure. For a relativistic electron beam, χ'_p diverges only when $p = 0$ in Eq. (5). Using $\chi'_p = \delta_{p0}\chi'_0$ in (10), one obtains

$$C_{nm} = U_{nm} + \chi'_0 V_{nm} \tag{11}$$

where

$$U_{nm} = \frac{-2\kappa_n}{W\Lambda_g(\delta_{n0}+1)}\tanh(\kappa_m D)\sum_{p=-\infty}^{\infty}\frac{\tanh(a_p G/2)}{\alpha_p}\Gamma_{pn}^-\Gamma_{pm}^+ \tag{12}$$

$$V_{nm} = \frac{-2\kappa_n}{W\Lambda_g(\delta_{n0}+1)}\tanh(\kappa_m D)\frac{\tanh(a_0 G/2)}{\alpha_0}\Gamma_{0n}^-\Gamma_{0m}^+ \tag{13}$$

In the absence of the electron beam, Vnm is ineffective in Eq. (11). We use MATLAB scripts to calculate the dispersion or band diagram for the symmetric Ez modes in a cold structure and plot it in Fig. 2 with the normalized frequency $\overline{a} = \omega/(cKg)$ in the vertical axis and the normalized propagation constant $\overline{k}_z = kz/Kg$ in the horizontal axis. In plotting Fig. 2, the following structure parameters are used for THz radiations, $\Lambda g = 50$ μm, $W = 30$ μm, $D = 60$ μm and $G = 150$ μm. Figure 2 clearly shows the distinct difference between a grating-waveguide FEL and an evanescent-mode Smith-Purcell radiator, because the latter does not have high-order frequency bands and the slope at the band edge is nonzero. An electron beam line with a slope β can be drawn on the same plot to find the synchronous points between the wave and the electron. For example, a 30-50 keV electron has a speed between 0.328c and 0.4122c. The beam line intercepts both the first and second band in the dispersion diagram. It is evident that the high-frequency bands offer the opportunity of generating high-frequency radiations. The condition $\overline{k}_z = 0.5\times$ m is known to be the Bragg condition of a grating along the grating-vector direction. As far as the first frequency band is concerned, the group velocity is positive or negative to the left or right of the Bragg line $\overline{k}_z = 0.5$, respectively. As analyzed by Swegle [5], such a negative-group-velocity device can function as a backward-wave oscillator when the beam current is above a certain threshold value. At the frequency where $\overline{k}_z = 0.5 \times$ m with m an integer, the group velocity of the wave is zero, because the distributed feedbacks from the gratings build up standing waves in the grating waveguide. If a beam

line intercepts the band curves at $\bar{k}_z = 0.5 \times m$, this grating-waveguide FEL behaves like an electron-driven, mirrorless DFB oscillator. The beam line in Fig. 2 has a beam energy of 31.36 keV, intercepting the Bragg resonance $\bar{k}_z = 0.5$ in the first band and a synchronous point in the second band. This grating-waveguide FEL thus can establish its oscillation at the Bragg resonance $\bar{k}_z = 0.5$ as long as the gain favours the DFB resonance.
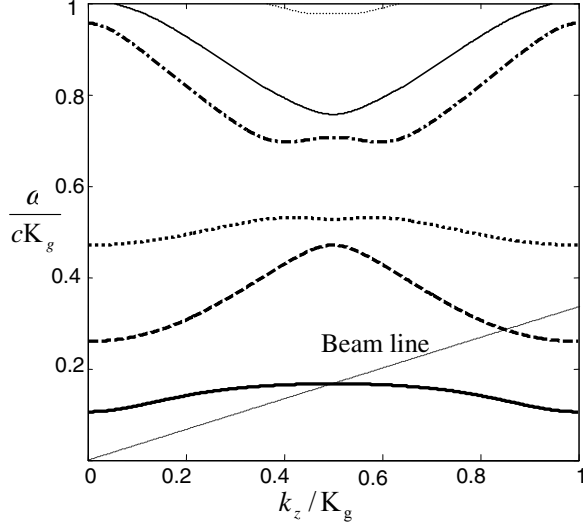
Figure 2: The band diagram of a grating waveguide with $\Lambda_g = 50$ μm, $W = 30$ μm, $D = 60$ μm and $G = 150$ μm. A 31.36 keV beam line intercepts the first band at the Bragg resonance, resulting in a low-threshold DFB oscillator.

GAIN CALCULATION

To calculate the small signal gain at a beam-wave synchronous point, we again used the perturbation technique described by Andrews *et al.* [4] to obtain

$$(k_z - k_0)^3 = \frac{\omega_p^2}{\gamma^3 \beta^2 c^2} \frac{V_{00}(\omega_0, k_0)}{U'_{00}(\omega_0, k_0)} \quad (14)$$

where k_0 is the synchronous wave number, $a_0 = \beta c k_0$,

$$U'_{00} = dU_{00} / dk_z, \quad (15)$$

and

$$V_{00} = \frac{2\kappa_0}{W\Lambda_g} \tanh(\kappa_0 D) \frac{\tanh(\alpha_0 \frac{G}{2})}{\alpha_0} \frac{\cos[(pK_g + k_z)W] - 1}{\alpha_p(pK_g + k_z)^2}. \quad (16)$$

The power gain e^{2gL} with g the gain coefficient and L the grating length can be calculated from the roots of Eq. (14), given by

$$g = \text{Im}[k_z - k_0] = \frac{\sqrt{3}}{2} \left| \frac{\omega_p^2}{\gamma^3 \beta^2 c^2} \frac{V_{00}(\omega_0, k_0)}{U_{00}'(\omega_0, k_0)} \right|^{1/3} \quad (17)$$

The plasma frequency ω_p^2 in the laboratory frame can be expressed as

$$\omega_p^2 = \frac{16c^2}{\beta d_x d_y} \frac{I_e}{I_A} \quad (18)$$

where I_A is Alfvén current, I_e is the electron beam current, d_x and d_y are the electron beam diameters in the x and y directions, respectively. With Eqs. (17, 18), the gain coefficient of a grating-waveguide FEL has cube-root dependence on the electron current. Figure 3 shows the gain coefficient as a function of the electron beam energy for a beam current of 5 mA and beam diameters of $d_x = d_y = 150$ μm. The continuous and dashed curves are plotted for synchronous points in the first and second bands of Fig. 2, respectively.
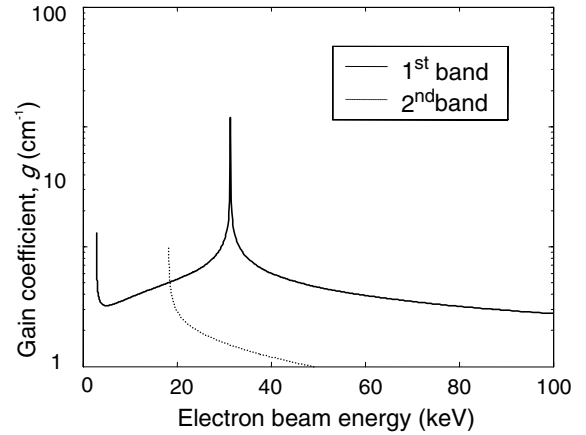
Figure 3: Small-signal gain coefficient of the symmetric E_z mode versus electron-beam energy for the first and second radiation bands. The gain coefficient diverges at the Bragg resonances.

In general the electron velocity is less than the velocity of light. For the first band, the gain coefficient diverges at the Bragg resonances $\bar{k}_z = 0.5$ and 1, corresponding to electron synchronous energies of 31.36 keV and 2.95 keV and radiation wavelengths of 298 μm and 469 μm, respectively. For the second band, the resonance at $\bar{k}_z = 0.5$ can not be used for beam-wave synchronization due to an unreasonable beam-line slope of $\beta > 1$ at the synchronous point. For the resonance point at $\bar{k}_z = 1$ in the second band, the electron beam energy is 18.6 keV, corresponding to a radiation wavelength of 183 μm. Therefore, given an electron beam energy, it is possible to generate a shorter radiation wavelength by resonating the radiation wave at the Bragg resonance in a high-order frequency band. This is a unique property that can not be offered by an evanescent-mode Smith-Purcell radiator.

A wave oscillator is characterized by a threshold gain at which the oscillator starts to oscillate. The above gain calculation is useful when one uses the grating-waveguide FEL as an amplifier. As mentioned previously, a grating

waveguide FEL can function as a BWO in the negative-slope portion of the dispersion curve or a DFB oscillator near the Bragg resonance. Following Swegle's analysis, Andrews *et al.* [6] has extended their model to calculate the starting current of a Smith-Purcell BWO. The same approach can be used to derive the starting current of the grating-waveguide BWO in a straightforward manner. However, finding the threshold current of a DFB grating-waveguide FEL is more complicated, although Miller *et al.* [7] has attempted it with limited success in comparing theory and experiment. If the grating corrugation is small compared with the waveguide gap, one can in principle decompose the oscillating field into the sum of a forward and a backward components, given by $H_x = H(y)[R(z)e^{-jk_{zz,0}z} + S(z)e^{jk_{zz,0}z}]$, where $H(y)$ is the transverse mode profile in an unperturbed waveguide, $R(z)$ and $S(z)$ are slowly varying field envelopes of the forward and backward components, respectively, and $k_{z,0}$ satisfies the Bragg condition $2k_{z,0} = mK_g$. The envelope fields satisfy the coupled-mode equations [8]

$$\frac{dR}{dz} = -j\delta R - j\kappa S + G(R, I) \qquad (19.a)$$

$$\frac{dS}{dz} = j\delta S + j\kappa^* R \qquad (19.b)$$

where $\delta = k_z - k_{z,0}$ is the detuning of k_z from the Bragg resonance, $G(R, I)$ is the forward gain function provided by the electron beam, and κ is the coupling coefficient between the forward and backward field components. The threshold current I_{th} and resonant k_z can be solved from the boundary condition of a diverging output under a finite input field. A detailed calculation will be presented in our subsequent publications.

DISCUSSION AND CONCLUSION

The grating waveguide is a slow-wave structure similar to a corrugated cylindrical waveguide used for a millimetre-wave BWO. Therefore a grating-waveguide FEL can function as a BWO when operating at the negative-slope portion of the dispersion curve. The main emphasis of this paper is to recognize the potential of using a grating-wave FEL as a low-threshold DFB oscillator at the Bragg resonance. The dispersion relation for a grating-waveguide FEL described by Eq. (9) can be reduced to that for an evanescent-mode Smith-Purcell radiator by letting the waveguide gap become a large number or $\alpha_p G/2 >> 1$. Although Andrews *et al.* [6] has noted that the gain of an evanescent-mode Smith-Purcell radiator diverges at the Bragg resonance, they claimed that the loss at the Bragg resonance always exceeds the gain. This claim was based on a model describing an electromagnetic energy propagating along a longitudinal direction of the device, which is not valid for a standing-wave resonator in which electromagnetic energy flows in both longitudinal directions and appears to have no net

group velocity in the resonator. Like a Fabry-Perot resonator, a DFB resonator is a standing-wave resonator and has been demonstrated in numerous applications. The Bragg resonance in an electron-pumped grating waveguide leading itself to a relativistic DFB laser was also not recognized by Schächter *et al.* [9], Kim *et al.* [10], Marshal *et al.* [2], and Killoran *et al.* [3] either, despite they all described electron radiations from variants of grating structures, including the Smith-Purcell radiator, the planar orotron, and the dual-grating resonator.

Unlike a BWO, a DFB oscillator can achieve a low threshold from significant distributed feedbacks in a properly designed grating waveguide. Since a grating-waveguide FEL operating at the Bragg resonance is virtually a DFB oscillator, the well known advantages associated with a DFB laser should hold true to a grating-waveguide FEL. Apart from its monolithic structure and mirrorless oscillation, the single-longitudinal-mode output from a grating-waveguide FEL will benefit the applications requiring high spectral purity of radiations.

REFERENCES

[1] J. Urata, M. Goldstein, M.F. Kimmitt, a. Naumov, C. Platt, J.E. Walsh, Phys. Rev. Lett. 80, (1998) 516.

[2] E. M. Marshall, P. M. Phillips, and J. E. Walsh, IEEE Trans. Plasma Science **16**, (1988) 199.

[3] J.H. Killoran, F.L. Hacker, and J. E. Walsh, IEEE Trans. on Plasma Science, vol. 22, No. 5, (1994) 530-535.

[4] H.L. Andrews, C. A. Brau, Phys. Rev. ST-AB **7** (2004) 070701.

[5] J. A. Swegle, Phys. Fluids **30** (4) (1987) 1201.

[6] H. L. Andrews, C. H. Boulware, C. A. Brau, and J. D. Jarvis, Phys. Rev. ST-AB **8** (2005) 050703.

[7] S. M. Miller, T. M. Antonsen, Jr., B. Levush, A. Bromborsky, D. K. Abe, and Y. Carmel, Phys. Plasmas **1** (3) (1994) 731.

[8] V. L. Bratman, G. G. Denisov, N. S. Ginzburg, and M. I. Petelin, IEEE J. Quan. Elec. QE-19 (1983) 282.

[9] L. Schächter, and A. Ron, Phys. Rev. A 40 (1989) 876.

[10] Kwang-Je Kim and Su-Bin Song, Nucl. Inst. Meth. A **475** (2001) 158-163.